Acta Crystallographica Section D
Biological Crystallography
ISSN 0907-4449

Cryophotolysis of caged compounds: a technique for trapping intermediate states in protein crystals

Thomas Ursby,[a,b]† Martin Weik,[c]‡ Emanuela Fioravanti,[a,b] Marc Delarue,[d] Maurice Goeldner[e] and Dominique Bourgeois[a,b]*

[a]LCCP, UMR 9015, Institut de Biologie Structurale, 41 Avenue Jules Horowitz, 38027 Grenoble CEDEX 1, France, [b]ESRF, 6 Rue Jules Horowitz, BP 220, 38043 Grenoble CEDEX, France, [c]Department of Crystal and Structural Chemistry, Bijvoet Center for Biomolecular Research, Utrecht University, Padualaan 8, NL-3584 CH Utrecht, The Netherlands, [d]Unité de Biochimie Structurale, Institut Pasteur, 28 Rue du Docteur Roux, 75724 Paris CEDEX 15, France, and [e]Laboratoire de Chimie Bioorganique, UMR 7514 CNRS, Faculté de Pharmacie, Université Louis Pasteur Strasbourg, BP 24, 67401 Illkirch CEDEX, France

† Present address: MAX-lab, Lund University, PO Box 118, S-22100 Lund, Sweden.
‡ Present address: LBM, UMR 9015, Institut de Biologie Structurale, 41 Avenue Jules Horowitz, 38027 Grenoble CEDEX 1, France.

Correspondence e-mail: bourgeoi@lccp.ibs.fr

Received 22 October 2001
Accepted 1 February 2002

PDB References: TMPK–TMP complex, 1gsi, r1gsisf; TMPK–TDP complex, 1gtv, r1gtvsf.

Caged compounds in combination with protein crystallography represent a valuable tool in studies of enzyme reaction intermediates. To date, photochemical triggering of reactions has been performed close to room temperature. Synchronous reaction initiation has only been achieved with enzymes of relatively slow turnover ($<0.1\ s^{-1}$) and caged compounds of high quantum yield. Here X-ray crystallography and microspectrophotometry were used to provide evidence that (nitrophenyl)ethyl (NPE) ester bonds can be photolyzed by UV light at cryotemperatures. NPE-caged ATP in flash-cooled crystals of *Mycobacterium tuberculosis* thymidylate kinase was photolyzed successfully at 100–150 K as assessed by the structural observation of ATP-dependent enzymatic conversion of TMP to TDP after temporarily warming the crystals to room temperature. A new method is proposed in which cryophotolysis combined with temperature-controlled protein crystallography can be used to trap reaction intermediates even in some of the fastest enzymes and/or when only compounds of low quantum yield are available. Raising the temperature after cryophotolysis may allow a transition barrier to be passed and an intermediate to accumulate in the crystal. A comparable method has only been used so far with proteins displaying endogenous photosensitivity. The approach described here opens the way to studying the reaction mechanisms of a much larger number of crystalline enzymes. Furthermore, it is shown that X-ray-induced radiolysis of caged compounds occurs if high-intensity synchrotron beamlines are used. This caveat should be taken into account when deriving data-collection protocols. It could also be used potentially as a way to trigger reactions.

1. Introduction

Crystallography can greatly contribute to the understanding of reaction mechanisms in enzymes through the observation of transient intermediate structures. Complementary to time-resolved crystallography at room temperature (Moffat, 1998), kinetic crystallography at low temperature (Moffat & Henderson, 1995; Schlichting, 2000) has opened new possibilities for following conformational changes in proteins. At low temperatures, enzyme-catalyzed reactions are slowed owing to a lack of thermal energy to overcome transition barriers along the reaction pathway and/or owing to modified physicochemical properties of the solvent (Fink & Petsko, 1981; Douzou & Petsko, 1984). They may even be blocked below temperatures associated with dynamical transitions (Frauenfelder *et al.*, 1979; Parak *et al.*, 1982; Doster *et al.*, 1989; Rasmussen *et al.*, 1992; Ferrand *et al.*, 1993). Some crystalline enzymes have a sufficiently slow turnover that intermediate

species may accumulate transiently at ambient temperature or at moderately low temperatures if proper solvents are used (Douzou & Petsko, 1984; Stoddard, 2001). These intermediates are then trapped by subsequent flash-cooling, thereby allowing data collection with standard monochromatic X-ray diffraction. However, this approach is inadequate when the turnover rate cannot be made much smaller than the rate of reaction initiation (*e.g.* the rate of substrate diffusion). In such cases, a more suitable method is to trigger at a temperature low enough to block the enzymatic reaction (typically 100–150 K; Weik *et al.*, 2001) and drive the formation of intermediate states by transiently delivering sufficient thermal energy to the sample. Although the question as to whether such cryo-intermediates are physiologically relevant should always be asked (Moffat & Henderson, 1995), this method appears to be more widely applicable than time-resolved crystallography using fast (Laue) data-collection protocols because it is technically easier and less demanding to crystals (Hajdu & Andersson, 1993; Scheidig *et al.*, 1999).

Triggering the reaction within the crystal at these temperatures (100–150 K) by diffusion of substrates, cofactors or even buffers cannot be envisaged easily. Instead, light can be used. This is why this method has only been applied to date to proteins displaying endogenous photosensitivity (Teng *et al.*, 1994; Genick *et al.*, 1998; Edman *et al.*, 1999; Chu *et al.*, 2000; Ostermann *et al.*, 2000; Royant *et al.*, 2000) or in cases where the X-rays themselves served as a trigger (Schlichting *et al.*, 2000). In this paper, we suggest that photolysis of caged compounds (Scheidig *et al.*, 1998) at temperatures too low for catalysis to proceed enables the use of the method to be extended to many light-insensitive enzymes, including the most rapid ones.

Caged compounds are photosensitive biologically inert precursors of molecules that are liberated in their active form upon irradiation with UV light (Kaplan *et al.*, 1978; McCray & Trentham, 1989; Corrie & Trentham, 1993). The reaction mechanisms of a number of enzymes have been studied using room-temperature photolysis of caged compounds followed by rapid Laue data collection (Schlichting *et al.*, 1990; Stoddard *et al.*, 1991, 1998; Goody *et al.*, 1992; Duke *et al.*, 1992, 1994). These experiments were possible because reaction rates were slow ($<0.1\ s^{-1}$) and because the high quality of the crystals allowed the use of a white X-ray beam and in some cases intense UV-light pulses. To eliminate the difficulties associated with the Laue technique, photolysis of caged GTP at 275 K has been combined recently with cryocrystallography of H-*ras* p21 (Scheidig *et al.*, 1999) and the structural picture of the reaction has been substantially improved. The photolysis could be performed close to room temperature because the reaction in the crystal was slow enough to achieve good synchronism with extended UV exposure (2–3 min). For faster enzymes whose turnover rate is incompatible with slow low-power photolysis of a caged compound (~30 s), photolysis at room temperature is inappropriate as short and intense UV-light pulses would have to be used, which may not be withstood by fragile crystals and may lead to incomplete photolysis. For the most rapid enzymes such as, for example, acetylcholinesterase (turnover rate of $20\,000\ s^{-1}$ in solution; Sussman *et al.*, 1991), this approach cannot be used because the turnover rate may exceed the maximum release rate of the caged compound or the achievable cooling rate of a protein crystal (>0.1 s; Teng & Moffat, 1998; Walker *et al.*, 1998), resulting in conformational heterogeneity throughout the crystal.

We have recently observed that photolysis of 1-(2-nitrophenyl)ethyl (NPE) caged arsenocholine and (deoxy)-thymidine monophosphate (TMP or thymidylate) does occur in flash-cooled amorphous solutions at 100 K (Specht *et al.*, 2001). Here, we used temperature-controlled crystallography and absorption microspectrophotometry to demonstrate photolysis at 100–150 K of caged ATP (NPE-ATP) in *M. tuberculosis* thymidylate kinase (TMPK*mt*) crystals. TMPK*mt* uses ATP as a phosphoryl donor to catalyze the reversible phosphorylation of TMP (Li de la Sierra *et al.*, 2001). We photolyzed caged ATP at 100–150 K and by subsequently warming the crystals to room temperature we allowed the released ATP to diffuse to the active site and the enzyme to phosphorylate the substrate. The observation at 2.3 Å resolution of the formation of the product (deoxy)-thymidine diphosphate (TDP) and of the corresponding structural changes of TMPK*mt* allowed us to validate the proposed method.

We also show here the possible radiolysis of NPE ester bonds by X-rays. This observation adds to the precautions that must be taken when working with caged compounds (McCray & Trentham, 1989; Barth *et al.*, 1997; Schlichting & Goody, 1997; Scheidig *et al.*, 1998). Alternatively, if carefully controlled, radiolysis by X-rays could serve as a tool to trigger reactions with caged compounds.

2. Materials and methods

2.1. *M. tuberculosis* thymidylate kinase

TMPK*mt* was co-crystallized with TMP as described in Li de la Sierra *et al.* (2000). To reduce the observed inhibition by sulfate ions at the ATP-binding site (Li de la Sierra *et al.*, 2001), crystals were transferred to a solution containing 40% PEG 2000, 10 m*M* ammonium sulfate, 0.1 *M* MES pH 6.0, 25 m*M* magnesium acetate, 2 m*M* β-mercaptoethanol. This solution also served as cryoprotectant and is referred to as the 'cryosolution'. 'Soaking solutions' were prepared by adding the substrate or caged substrate, as well as 3 m*M* EDTA and 1.5 m*M* DTT, to the cryosolution (see below). Crystals were transferred and manipulated with nylon loops (Hampton Research, Laguna Niguel, California, USA).

2.2. TMPK*mt*–TMP and TMPK*mt*–TDP crystals

The crystal (~160 × 160 × 320 µm) used for determining the TMPK*mt*–TMP structure was soaked in the cryosolution for 2 min prior to being flash-cooled in liquid nitrogen. A crystal of approximately the same size was used to determine the TMPK*mt*–TDP structure. The crystal was soaked in the cryosolution for 21 h and then for 20 h in a drop of soaking

solution containing 7 m*M* ATP before being flash-cooled in liquid nitrogen.

2.3. Crystals used for photolysis and radiolysis experiments

All manipulations of caged compounds were performed under filtered light (longpass filter 410 nm, Kodak Gelatin filter Wratten 2A). NPE-ATP was purchased from Molecular Probes (Eugene, OR, USA). Crystals (∼70 × 70 × 140 µm) were quickly washed in a 5 µl drop of the cryosolution and then soaked for 24–62 h in drops of soaking solution containing 8 m*M* TMP and 12 m*M* NPE-ATP. The crystals were then washed in three consecutive 5 µl drops of the cryosolution (total time ∼30 s) to remove all caged ATP surrounding the crystal before being flash-cooled to 150 K in a nitrogen stream (Oxford Cryosystems, Oxford) and mounted on a microspectrophotometer setup (see below). By measuring an absorption spectrum, it was verified that the solution surrounding the crystals in the loops did not contain any residual caged ATP. Crystals were photolyzed using a xenon flashlamp (Rapp OptoElectronic, Hamburg, Germany), with 25 flashes of ∼1 ms duration and 20 mJ mm^{-2} delivered at a 1 Hz frequency. The spectrum from the lamp peaked at 325 nm with a 37% bandwidth. The crystals were then warmed to room temperature and left in 5 µl drops of cryosolution for ∼20 s, ∼1 min or ∼1 h before being recooled to 100 K in a nitrogen stream. The control crystals were treated identically but without being exposed to UV flashes. In separate experiments, crystals were photolyzed at 100 K or, using a low-power (0.75 mW/0.01 mm^2) 355 nm laser (Nanolase, Meylan, France), at 150 K. Crystals soaked for 70 h in a soaking solution with 15 m*M* NPE-TMP were used for measurements of the radiolysis by X-rays. NPE-TMP was synthesized and kindly provided by Serge van Calenbergh, University of Leuven, Belgium.

Table 1
Data-collection statistics.

Values in parentheses refer to the highest resolution shell. The data set (or crystal) numbers refer to the list in Table 3. All crystals belong to the space group $P6_522$, with unit-cell parameters $a = b = 76.5$, $c = 134.5$ Å.

Data set name and number	TMP, data set 1	TDP, data set 2	20 s, data set 3	1 min, data set 4	1 h, data set 5	Control, data set 9
Substrate†	—	ATP	NPE-ATP	NPE-ATP	NPE-ATP	NPE-ATP
Photolysis temperature (K)	—	—	150	150	150	—
Reaction time‡	—	—	20 s	1 min	1 h	1 h
Wavelength (Å)	0.75	0.93	0.75	0.93	0.75	0.75
Resolution (Å)	1.6	1.55	2.0	2.0	2.3	2.1
No. of observations	252502	360419	56700	57200	28377	47149
No. of unique reflections	30736	33359	16102	16494	10310	13302
Completeness (%)	99.1 (98.5)	97.5 (96.0)	99.5 (99.3)	99.7 (99.3)	96.3 (87.1)	94.5 (86.5)
Redundancy	8.2 (5.4)	10.8 (6.7)	3.5 (3.5)	3.5 (3.5)	2.8 (2.0)	3.5 (2.4)
R_{sym}§ (%)	7.6 (28.2)	6.5 (17.9)	5.6 (28.3)	5.3 (30.0)	6.5 (30.7)	8.3 (26.0)
$\langle I/\sigma(I)\rangle$	20.2 (4.3)	26.2 (9.0)	16.5 (4.7)	18.3 (3.8)	13.9 (2.5)	11.4 (3.2)

† All crystals were grown in the presence of TMP. ‡ The time the crystals were left at room temperature after photolysis. § R_{sym} increases above 20% for data sets 1, 3, 4, 5 and 9 at 1.75, 2.1, 2.1, 2.5 and 2.3 Å, respectively.

Table 2
Refinement statistics for the TMPK*mt*–TMP and TMPK*mt*–TDP crystals.

Crystal 2 contained 48% TMPK*mt*–TDP molecules and 52% TMPK*mt*–TMP molecules according to the refinement (see §2). Values in parentheses refer to the highest resolution shell.

	TMPK*mt*–TMP, data set 1	TMPK*mt*–TDP, data set 2
R_{cryst} (%)	19.3 (23.1)	19.2 (20.6)
R_{free} (%)	21.0 (25.9)	20.9 (23.4)
No. of protein atoms†	1535 + 153	1535 + 349
No. of water molecules	243	269 + 22‡
No. of other atoms§	44	48 + 32‡
No. of atoms in TMP conformation	—	280
Average *B* factors (Å^2)		
Overall	22.4	20.8
Protein atoms	20.4	18.5
Nucleotides and ions	20.3	17.1
Solvent	37.1	36.5
Ramachandran plot, residues in		
Most favoured regions (%)	95.0	95.5
Additional allowed regions (%)	4.4	3.9
Disallowed regions (%)	0.6	0.6

† The second value corresponds to the number of atoms in alternate conformations. For data set 2 these include the residues modelled in both TMPK*mt*–TMP and TMPK*mt*-TDP conformations. ‡ The second value corresponds to atoms in the TMPK*mt*–TMP conformation. § TMP/TDP and SO_4^{2-}, Mg^{2+} and acetate ions.

2.4. Microspectrophotometry

A microspectrophotometer setup was used for spectral analysis. Light from a deuterium light source (Oriel, Stratford, Connecticut, USA) was focused onto the crystal (focal spot ∼30 µm) *via* an optical fibre. The transmitted light was analyzed using a CCD spectrometer (Ocean Optics, Dunedin, Florida, USA) providing a 200–850 nm wavelength range.

2.5. X-ray data collection and analysis

All diffraction data were collected at 100 K at beamlines ID9, ID14-2 or ID14-3 at ESRF, Grenoble, France and were processed with *DENZO* (Otwinowski & Minor, 1997) and *SCALA* (Collaborative Computational Project, Number 4, 1994). Data-collection statistics are shown in Table 1. The models were refined with *CNS* (Brünger *et al.*, 1998). Difference electron-density maps were weighted to optimize the signal-to-noise ratio (Ursby & Bourgeois, 1997).

A 1.6 Å model of the TMPK*mt*–TMP complex was refined using diffraction data from crystal 1 (Table 1) and the structure of Li de la Sierra *et al.* (2001) as a starting model. A 1.55 Å model of the TMPK*mt*–TDP complex was refined using diffraction data from crystal 2 and the TMPK*mt*–TMP structure as a starting model in which only the amino acids were included. Initial refinement led to the observation that in this crystal a significant fraction of the molecules contained unconverted TMP. To account for this, the parts of the structure that showed significant electron difference density relative to the TMPK*mt*–TMP structure were modelled with two conformations representing the TMPK*mt*–TDP and the TMPK*mt*–TMP structures. The TMPK*mt*–TMP conformation

Table 3
Refinement of the fraction of TMPK molecules with TDP bound.

Data set No.	Crystal soaked with	Photolyzed	Time at RT	d_{min} (Å)	Fraction TDP
1	—	—	—	1.6	0.01
2	ATP	—	—	1.55	0.48
3	NPE-ATP	Yes (150 K)	20 s	2.0	0.17
4	NPE-ATP	Yes (150 K)	1 min	2.0	0.24
5	NPE-ATP	Yes (150 K)	1 h	2.3	0.38
6	NPE-ATP	Yes (150 K)†	1 h	2.5	0.40
7	NPE-ATP	Yes, laser (150 K)†	1 h	2.3	0.30
8	NPE-ATP	Yes (100 K)†	1 h	2.6	0.37
9	NPE-ATP	No	1 h	2.1	0.09
10	NPE-ATP	No†	1 h	2.4	0.11

† Data-collection statistics not shown.

was kept fixed during the refinement and included 29 amino acids, one TMP molecule, two sulfate ions and 22 water molecules. The TMPK*mt*–TDP conformation included the same amino acids and sulfate ions, one TDP molecule and 20 water molecules. The occupancy of the two conformations, as well as the positions and *B* factors of the TMPK*mt*–TDP conformation were refined iteratively together with the refinement of the remaining parts of the structure. Refinement statistics for the TMPK*mt*–TMP and TMPK*mt*–TDP models are found in Table 2.

The degree of conversion from TMP to TDP in the crystals containing NPE-ATP (crystals 3–10, Table 3) was estimated by refining the occupancies of a TDP conformation (including TDP and Tyr39) *versus* a TMP conformation (including TMP, Tyr39 and one water molecule at the position of the β-phosphate of TDP). The occupancy refinement was performed with these parts since at the available resolution (see Table 3) they delineate the location where significant difference electron density was found.

3. Results

As a first step to establish the validity of the proposed method, we demonstrated the activity of the enzyme in the crystalline form. A model of the TMPK*mt*–TMP complex was first refined to 1.6 Å resolution, which essentially confirmed the 1.95 Å model of Li de la Sierra *et al.* (2001) (Tables 1 and 2). In a second experiment, we transferred crystals to a solution

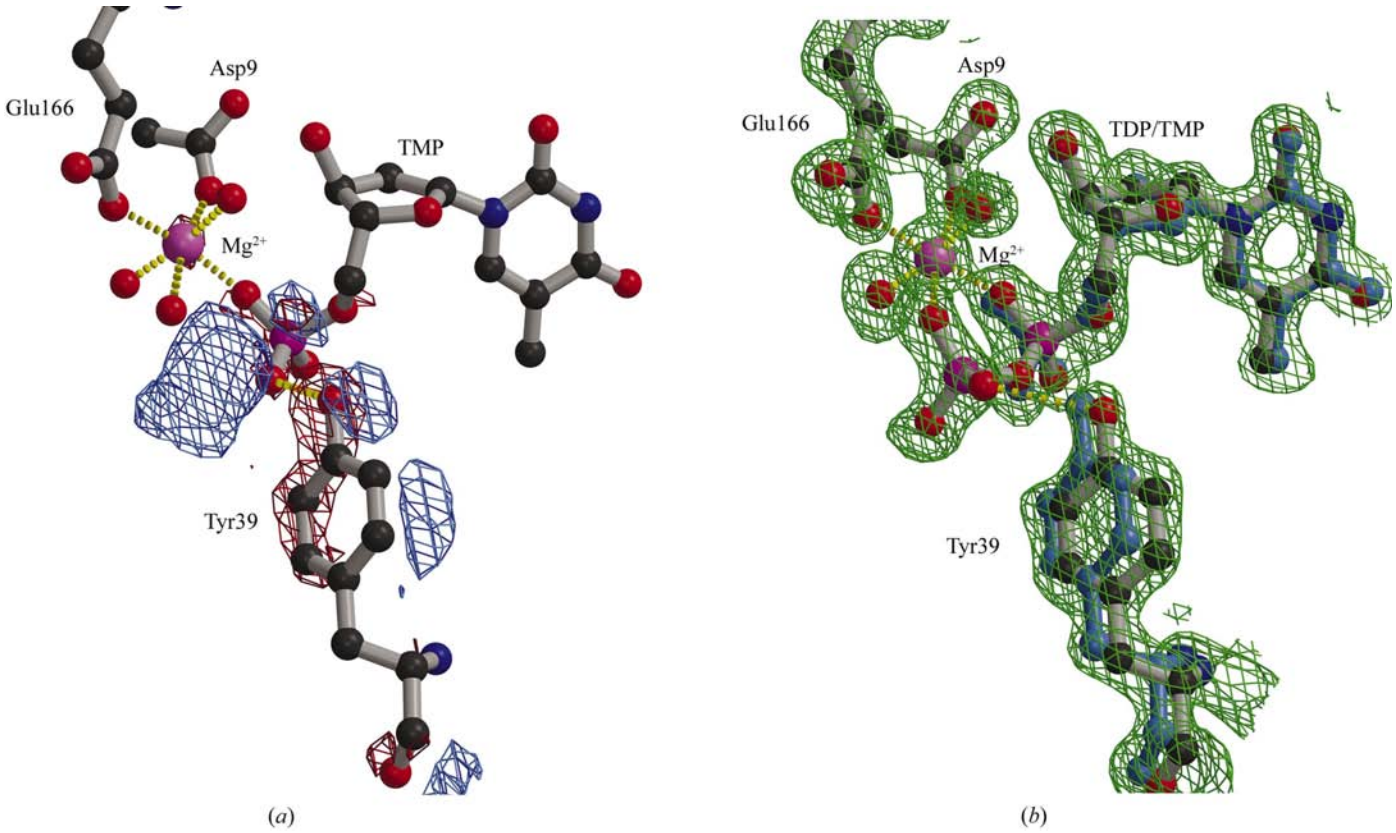

Figure 1
(*a*) Difference map between data set 2 and data set 1 contoured at $\pm 5\sigma$ (blue corresponds to density appearing in data set 2 and red to density disappearing compared with data set 1). The refined TMPK*mt*–TMP model shown in the figure was used for phase calculation. (*b*) A $2F_o - F_c$ simulated-annealing omit map of data set 2 contoured at 1σ. The TDP molecule, Tyr39 and the Mg^{2+} ion with its ligands (Glu166, Asp9 and two water molecules) from the TMPK*mt*–TDP model are shown as grey sticks, while the TMP molecule and Tyr39 from the TMPK*mt*–TMP model are shown in blue. The nucleotides, Tyr39, Mg^{2+} and all atoms within 3.5 Å were omitted in the phase calculation. Both the density of the TDP β-phosphate and the motion of Tyr39 resulting from the conversion of TMP to TDP are clear at this high resolution (1.55 Å), even though crystal 2 is a mixture containing 52% TMPK*mt*–TMP, as indicated by the omit map density of Tyr39 that covers both conformations. Figures were prepared with *BOBSCRIPT* (Esnouf, 1999) and *Raster3D* (Merritt & Bacon, 1997).

containing ATP. A new density was observed next to the phosphate group of the TMP molecule that could unambiguously be assigned to the second phosphate of a TDP molecule (Fig. 1). The corresponding X-ray structure determined to 1.55 Å resolution (Tables 1 and 2) proves that the enzyme is active in the crystal. In this structure, despite the low concentration of ammonium sulfate in the cryosolution, a sulfate ion is still observed with high occupancy at the putative binding site of the β-phosphate of ATP (Li de la Sierra *et al.*, 2001) and ADP is not visible. We concluded that ATP molecules could bind transiently to the active site and donate their γ-phosphate to TMP. The refined structure consists of a mixture of 48% TMPK*mt*–TDP and 52% TMPK*mt*–TMP. The incomplete conversion to TDP probably results from the moderate concentration of ATP used and from the establishment of a chemical equilibrium resulting from ADP retention within the protein matrix (Silhavy *et al.*, 1975). The limited ATP concentration served to avoid the additional formation of TTP also shown to be catalyzed from TDP by the enzyme (A. Haouz & E. Fioravanti, personal communication). A characterization of the enzymology and structural changes taking place in TMPK*mt* crystals will be reported elsewhere.

Attempts to obtain crystals of either a TMPK*mt*–NPE-TMP or a TMPK*mt*–NPE-ATP complex were unsuccessful. However, absorption spectroscopy showed that crystals of TMPK*mt*–TMP soaked in NPE-ATP (or NPE-TMP) and carefully rinsed contained the caged compound, presumably in the solvent channels. It also suggested complete photolysis at 150 K using a xenon flashlamp (Fig. 2).

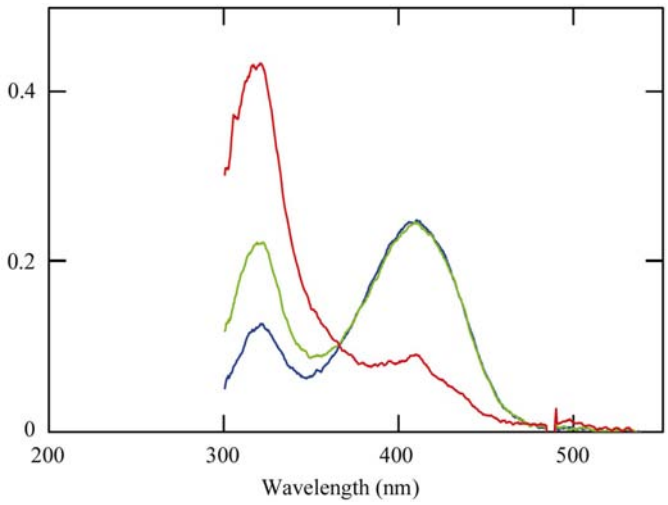

Figure 2
Difference spectra as a function of number of UV flashes of crystal 5 soaked with caged ATP and photolyzed at 150 K (blue, green and red corresponds to one, two and ten flashes, respectively). After ten flashes the difference spectrum was stable, indicating complete photolysis. The peak around 320 nm is characteristic of the released nitrosoacetophenone group. The broad peak around 400 nm probably arises from an aci-nitro intermediate appearing after photon absorption and before the release of the cage (Specht *et al.*, 2001). The peak around 400 nm after ten flashes is characteristic of photolyzed crystals, even when no caged compound is present, and probably arises from damage to the protein. It is not present in the spectra of crystals photolyzed with the 355 nm laser.

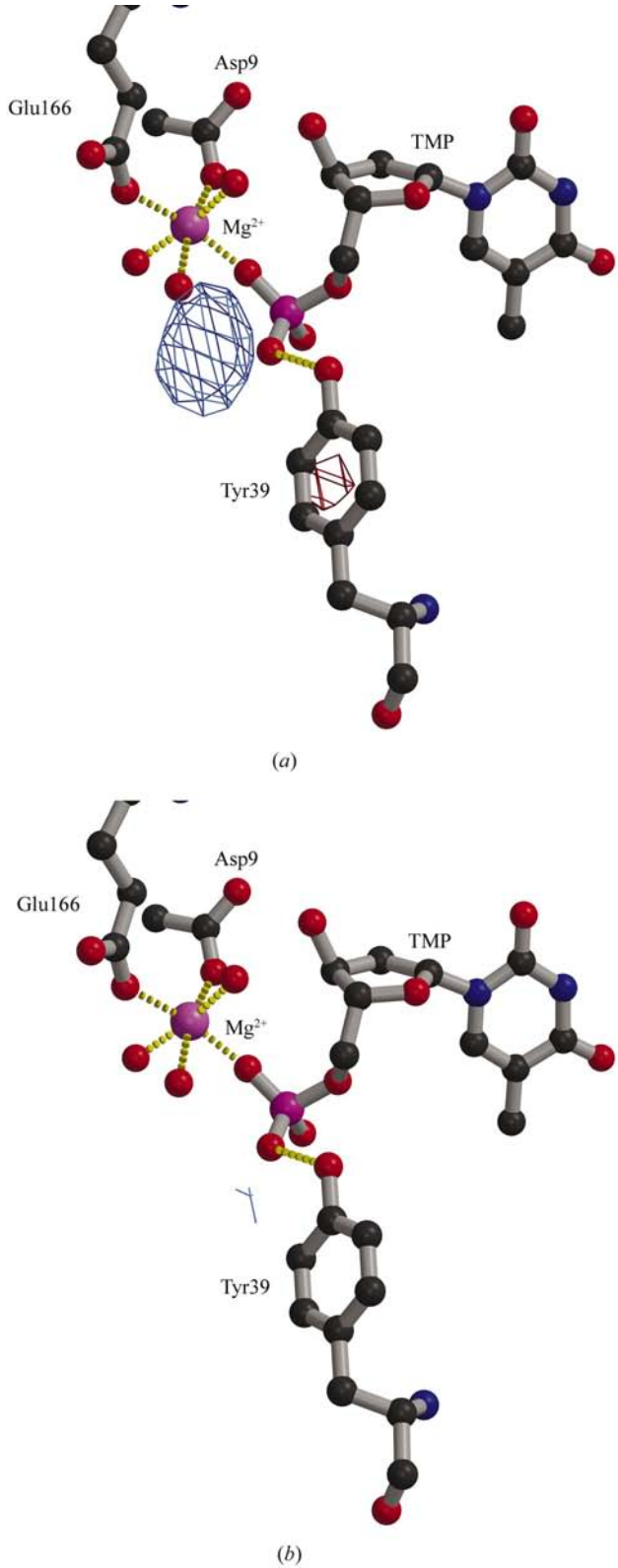

Figure 3
(*a*) Difference map between data set 5 (a crystal with caged ATP photolyzed at 150 K and then left at room temperature for 1 h before data collection) and data set 1 (TMPK*mt*–TMP). (*b*) Difference map between data set 9 (a crystal treated in exactly the same way as for data set 5 but not photolyzed) and data set 1. The maps are contoured at $\pm 5\sigma$. Blue corresponds to density appearing on photolysis and red to density disappearing on photolysis.

After cryophotolysis of NPE-ATP, crystals were transferred to drops deprived of substrates and left at room temperature for 1 h before being remounted at 100 K to collect X-ray data. The resulting electron-density maps showed that a significant fraction of TMP has been transformed to TDP (Fig. 3*a*). In control experiments, similar crystals were treated identically but were not exposed to UV flashes. The corresponding maps showed that no TDP had been formed (Fig. 3*b*). The experiment was repeated with consistent results (Table 3).

Assuming complete photolysis of NPE-ATP, an occupancy of ∼40% was expected for TDP if all released ATP molecules bind to an enzyme molecule and react and if the back reaction is neglected (the rinsed crystals contained 29 m*M* enzyme but only 12 m*M* NPE-ATP). This estimation agrees well with our results (Table 3). A similar occupancy for TDP was observed when the photolysis was performed at 100 K (a temperature well below the glass-transition temperature of solvent in protein crystals; Weik *et al.*, 2001) and a slightly lower one when the photolysis was performed at 150 K with a low-power 355 nm laser (Table 3). However, when the crystal was left at room temperature after photolysis for a shorter time, the occupancy of the TMPK*mt*–TDP complex was reduced (Table 3), suggesting a rate of TDP formation within the crystal of $\sim 0.01\ s^{-1}$. In the control experiments the occupancy of the TMPK*mt*–TDP complex refined to ∼10% (Table 3). This could arise from a small amount of TDP or ATP initially present and/or to inaccuracies in the refinement protocol.

It was observed that TMPK*mt* crystals soaked with NPE-TMP or NPE-ATP did not show the expected spectral changes associated with cage release when exposed to UV light *after* X-ray data collection. In order to assess the possibility of radiolysis by X-rays, absorption spectra were measured before and after X-ray data collection of an unphotolyzed crystal of TMPK*mt* soaked with NPE-TMP (Fig. 4). The overall shape of the spectra indicates the appearance after data collection of a broad double peak around 300 nm, characteristic of the released cage. Additionally, UV exposure after data collection did not further increase this peak. This behaviour was observed for several crystals and suggests complete radiolysis by X-rays.

4. Discussion

Our results unambiguously show that photolysis of caged compounds in protein crystals is feasible at temperatures as low as 100 K and can be combined with temperature-controlled crystallography to follow the progress of enzymatic reactions.

The exact mechanism by which the *ortho*-nitrosoacetophenone cage is released at cryotemperatures remains unclear, since the Arrhenius behaviour of the photofragmentation reaction of NPE compounds suggests a rate constant of $10^{-16}\ s^{-1}$ at 100 K and pH 6 (Barabás & Keszthelyi, 1984). However, local heating is likely to occur upon UV photon absorption, which may serve to carry forward the fragmentation reaction without significantly affecting the overall temperature of the crystal (Specht *et al.*, 2001).

The proposed method opens the way for new experiments to trap intermediate structures of enzymes, including the most rapid ones. Moreover, caged compounds of low quantum yield may be used (McCray & Trentham, 1989), since at cryotemperatures the rate of photolysis is not an issue. Enzymes for which there are no compounds of high quantum yield available could therefore be studied. For example, caged dioxygen (MacArthur *et al.*, 1995), which displays a quantum yield of 0.04 at physiological pH, could serve to study the mechanisms of many dioxygenases. Caged protons (Khan *et al.*, 1993) could also be used to trigger pH-dependent catalytic activity at low temperature.

The method applies when the caged compound binds prior to photolysis or when it has low affinity for the active site (Cohen *et al.*, 1997; Scheidig *et al.*, 1998). In the latter case, the system must be brought after cryophotolysis to a temperature that permits diffusion of the uncaged high-affinity compound from the solvent channels into the active site. This is expected to occur just above the glass-transition temperature (Smith & Kay, 1999) for small molecules such as dioxygen (MacArthur *et al.*, 1995) or protons (Khan *et al.*, 1993) and possibly also for larger molecules such as ATP. In the former case, the temperature increase may need to allow the released cage to diffuse out of the active site.

The design of suitable temperature profiles allowing the surmounting of transition barriers along the reaction pathway is of crucial importance to the success of such experiments. The accessible temperature range might be restricted by caveats such as crystal tolerance or ice formation. To facilitate

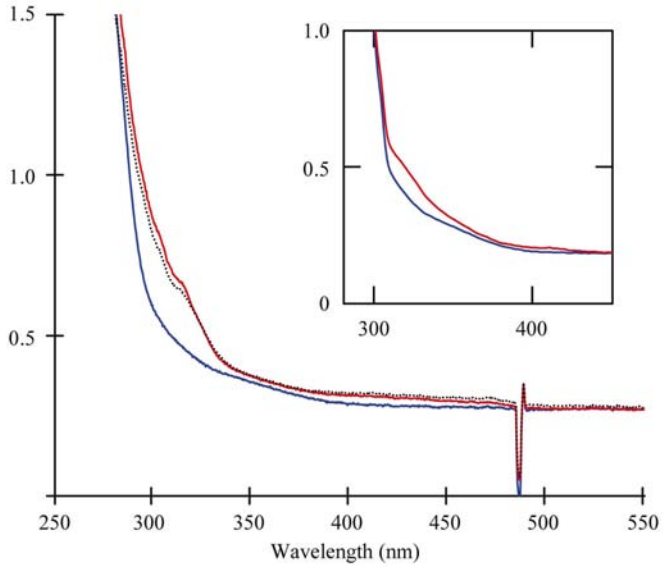

Figure 4
Spectra before (blue) and after (red) data collection of a crystal soaked with caged TMP. The crystal was subsequently exposed to UV light (dotted black curve). The inset shows a crystal soaked with caged TMP before (blue) and after (red) exposure to UV light. The changes arising from X-ray exposure are similar to the changes arising from UV exposure. Furthermore, the X-ray-exposed crystal does not show these changes when exposed to UV light. Since the spectra before and after data collection were measured with the crystal in different positions, the difference is not very accurate.

this design, microspectrophotometry of coloured crystals (Royant *et al.*, 2000) or X-ray techniques (Weik *et al.*, 2001) may be used to reveal conformational changes or transitions in solvent structure and dynamics as the temperature is varied. For relatively slow enzymes, transient heating to room temperature can be sufficient to achieve good synchronization throughout the crystal.

It is now recognized that X-rays not only degrade the overall quality of protein crystals, but may also specifically alter chemical structures such as disulfide bridges or carboxylic groups (*e.g.* Weik *et al.*, 2000; Burmeister, 2000; Ravelli & McSweeney, 2000). The present study shows that UV-sensitive compounds such as *ortho*-nitrobenzyl derivatives may also be affected by X-rays, although the mechanism by which this occurs remains unclear. This complication has not always been observed (Stoddard *et al.*, 1998), suggesting that radiolysis by X-rays might depend on X-ray dose or dose rate, or on the specific structure of the caged compound. Nevertheless, this difficulty should be investigated in all cases. Even when quick photolysis is required, *e.g.* when photolysis and data collection is performed at room temperature, it is important to photolyze the caged compounds completely by UV light prior to X-ray exposure in order to avoid further radiolysis by X-rays that would induce the build-up of a mixture of structural states in the crystal. X-rays could also be used deliberately to release the cage (Schlichting *et al.*, 2000) at cryotemperature prior to data collection, at the expense of other potential structural damage.

The strategy we used was necessary to circumvent the difficulties associated with X-ray-induced radiolysis of NPE-ATP and protein radiation damage. Collecting only one data set per crystal at 100 K minimized the effects of secondary radiation damage, whereas observing ATP release indirectly through the measurement of TDP formation allowed the decoupling of UV photolysis from X-ray radiolysis. Indeed, radiolysis by X-rays could not lead to TDP formation since the temperature was kept at 100 K during data collection, a temperature at which the enzymatic activity of TMPK*mt* is blocked. This is why the control experiments performed under exactly the same conditions but without UV photolysis showed negligible levels of TDP formation. The build-up of TDP after cryophotolysis of NPE-ATP also proved that the potential side-reactions associated with the release of the nitrosoacetophenone cage did not block the catalytic activity of crystalline TMPK*mt*.

In the case of TMPK*mt*, the chosen temperature profile did not allow us to observe any intermediate state accumulating within the crystal because binding of ATP to the active site is rate limiting at room temperature under the present crystallization conditions. Cryophotolysis followed by transient heating to a moderately low temperature in which the solvent is fluid could possibly offer new chances to trap intermediate structures. However, the overall strategy we have used provides a general framework for future studies on various possibly faster enzymes.

Despite the rather slow rate of TDP formation within crystals of TMPK*mt* at ambient temperature, a substantial amount of TDP was already observed after 20 s (Table 3). If NPE-ATP photolysis had been performed at ambient temperature, rapid, powerful and harmful UV-light pulses would have been required to preserve optimal synchronization throughout the crystal. Instead, by working at cryotemperatures, the photolysis duration was not an issue and the damaging effects of UV light could be diminished by delivering a large number of low-power pulses to the crystal at a low frequency. Low-power laser light at, for example, 355 nm appears even more favourable for future studies, since at this wavelength absorption by aromatic amino acids is greatly reduced, leading to reduced damage and potentially also to more homogeneous photoactivation. This is in general not possible at room temperature since the quantum yield must be maximized to achieve rapid and efficient photolysis. When using a 355 nm laser we did not observe the development of a peak at around 400 nm (red curve, Fig. 2) nor residual spectral distortions (not shown) which may tentatively be assigned to the development of radiation damage. Cryophotolysis could also be envisaged by two-photon absorption using light in the range 640–700 nm (Denk *et al.*, 1990).

In conclusion, the possibility of photolyzing caged compounds at cryotemperatures adds an additional tool to the panel of methods based on cryocrystallography (Moffat & Henderson, 1995; Schlichting, 2000) that allow trapping of intermediate states in protein crystals. In particular, it opens the way to the study of rapid structural changes in enzymes, a field that was hitherto reserved to a limited number of proteins displaying endogenous photosensitivity. Experiments can also be designed to study global protein dynamics and/or dynamical transitions at low temperature (Frauenfelder *et al.*, 1979; Parak *et al.*, 1982; Doster *et al.*, 1989; Rasmussen *et al.*, 1992; Ferrand *et al.*, 1993). Photolysis in the range 100–150 K allows the use of gentle light sources, therefore contributing to the preservation of crystal quality (Weik *et al.*, 2001). A wide range of caged compounds can benefit from the technique, including those that are moderately photosensitive.

We thank Serge van Calenbergh, University of Leuven for synthesis of NPE-TMP, Ahmed Haouz, Pasteur Institute for enzymatic studies of TMPK*mt* and Hélène Munier-Lehmann, Pasteur Institute for providing the purified TMPK*mt* enzyme. This work was supported by the EU Biotechnology program BIO4-CT98-0354. MW was supported by an EMBO long-term fellowship and is grateful to J. Kroon, P. Gros, I. Silman and J. Sussman for many fruitful discussions.

References

Barabás, K. & Keszthelyi, L. (1984). *Acta Biochim. Biophys. Acad. Sci. Hung.* **19**, 305–309.

Barth, A., Corrie, J. E. T., Gradwell, M. J., Maeda, Y., Matele, W., Meier, T. & Trentham, D. R. (1997). *J. Am. Chem. Soc.* **119**, 4149–4159.

Brünger, A. T., Adams, P. D., Clore, G. M., DeLano, W. L., Gros, P., Grosse-Kunstleve, R. W., Jiang, J.-S., Kuszewski, J., Nilges, M., Pannu, N. S., Read, R. J., Rice, L. M., Simonson, T. & Warren, G. L. (1998). *Acta Cryst.* D**54**, 905–921.

Burmeister, W. P. (2000). *Acta Cryst.* D**56**, 328–341.
Chu, K., Vojtchovský, J., McMahon, B. H., Sweet, R. M., Berendzen, J. & Schlichting, I. (2000). *Nature (London)*, **403**, 921–923.
Cohen, B. E., Stoddard, B. L. & Koshland, D. E. Jr (1997). *Biochemistry*, **36**, 9035–9044.
Collaborative Computational Project, Number 4 (1994). *Acta Cryst.* D**50**, 760–763.
Corrie, J. E. T. & Trentham, D. R. (1993). *Bioorganic Photochemistry*, Vol. 2, *Biological Applications of Photochemical Switches*, edited by H. Morrison, pp. 243–299. New York: Wiley.
Denk, W., Strickler, J. H. & Webb, W. W. (1990). *Science*, **248**, 73–76.
Doster, W., Cusack, S. & Petry, W. (1989). *Nature (London)*, **337**, 754–756.
Douzou, P. & Petsko, G. A. (1984). *Adv. Protein Chem.* **36**, 245–361.
Duke, E. M. H., Hadfield, A., Walters, S., Wakatsuki, S., Bryan. R. K. & Johnson, L. N. (1992). *Philos. Trans. R. Soc. London Ser. A*, **340**, 245–261.
Duke, E. M., Wakatsuki, S., Hadfield, A. & Johnson L. N. (1994). *Protein Sci.* **3**, 1178–1196.
Edman, K., Nollert, P., Royant, A., Belrhali, H., Pebay-Peyroula, E., Hajdu, J., Neutze, R. & Landau, E. M. (1999). *Nature (London)*, **401**, 822–826.
Esnouf, R. M. (1999). *Acta Cryst.* D**55**, 938–940.
Ferrand, M., Dianoux, A. J., Petry, W. & Zaccai, G. (1993). *Proc. Natl Acad. Sci. USA*, **90**, 9668–9672.
Fink, A. L. & Petsko, G. A. (1981). *Adv. Enzymol. Relat. Areas. Mol. Biol.* **52**, 177–246.
Frauenfelder, H., Petsko, G. A. & Tsernoglou, D. (1979). *Nature (London)*, **280**, 558–563.
Genick, U. K., Soltis, S. M., Kuhn, P., Canestrelli, I. L. & Getzoff, E. D. (1998). *Nature (London)*, **392**, 206–209.
Goody, R. S., Pai, E. F., Schlichting, I., Rensland, H., Scheidig, A., Franken, S. & Wittinghofer, A. (1992). *Philos. Trans. R. Soc. London Ser. B*, **336**, 3–10.
Hajdu, J. & Andersson, I. (1993). *Annu. Rev. Biophys. Biomol. Struct.* **22**, 467–498.
Kaplan, J. H., Forbush, B. & Hoffman, J. F. (1978). *Biochemistry*, **17**, 1929–1935.
Khan, S., Castellano, F., Spudich, J. L., McCray, J. A., Goody, R. S., Reid, G. P. & Trentham, D. R. (1993). *Biophys. J.* **65**, 2368–2382.
Li de la Sierra, I., Munier-Lehmann, H., Gilles, A. M., Bârzu, O. & Delarue, M. (2000). *Acta Cryst.* D**56**, 226–228.
Li de la Sierra, I., Munier-Lehmann, H., Gilles, A. M., Bârzu, O. & Delarue, M. (2001). *J. Mol. Biol.* **311**, 87–100.
MacArthur, R., Sucheta, A., Chong, F. F. & Einarsdottir, O. (1995) *Proc. Natl Acad. Sci. USA*, **92**, 8105–8109.
McCray, J. A. & Trentham, D. R. (1989). *Annu. Rev. Biophys. Biophys. Chem.* **18**, 239–270.
Merritt, E. A. & Bacon, D. J. (1997). *Methods Enzymol.* **277**, 505–524.
Moffat, K. (1998). *Nature Struct. Biol.* **5**, Suppl., 641–643.
Moffat, K. & Henderson, R. (1995). *Curr. Opin. Struct. Biol.* **5**, 656–663.
Ostermann, A., Waschipky, R., Parak, F. G. & Nienhaus, G. U. (2000). *Nature (London)*, **404**, 205–208.
Otwinowski, Z. & Minor, W. (1997). *Methods Enzymol.* **276**, 307–326.
Parak, F., Knapp, E. W. & Kucheida, D. (1982). *J. Mol. Biol.* **161**, 177–194.
Rasmussen, B. F., Stock, A. M., Ringe, D. & Petsko, G. A. (1992). *Nature (London)*, **357**, 423–424.
Ravelli, R. B. & McSweeney, S. M. (2000). *Structure Fold. Des.* **8**, 315–328.
Royant, A., Edman, K., Ursby, T., Pebay-Peyroula, E., Landau, E. M. & Neutze, R. (2000). *Nature (London)*, **406**, 645–648.
Scheidig, A. J., Burmester, C. & Goody, R. S. (1998). *Methods Enzymol.* **291**, 251–264.
Scheidig, A. J., Burmester, C. & Goody, R. S. (1999). *Structure Fold. Des.* **7**, 1311–1324.
Schlichting, I. (2000). *Acc. Chem. Res.* **33**, 532–538.
Schlichting, I., Almo, S. C., Rapp, G., Wilson, K., Petratos, K., Lentfer, A., Wittinghofer, A., Kabsch, W., Pai, E. F. & Petsko, G. A. (1990). *Nature (London)*, **345**, 309–315.
Schlichting, I., Berendzen, J., Chu, K., Stock, A. M., Maves, S. A., Benson, D. E., Sweet, R. M., Ringe, D., Petsko, G. A. & Sligar, S. G. (2000). *Science*, **287**, 1615–1622.
Schlichting, I. & Goody, R. S. (1997). *Methods Enzymol.* **277**, 467–490.
Silhavy, T. J., Szmelcman, S., Boos, W. & Schwartz, M. (1975). *Proc. Natl Acad. Sci. USA*, **72**, 2120–2124.
Smith, R. S. & Kay, B. D. (1999). *Nature (London)*, **398**, 788–791.
Specht, A., Ursby, T., Weik, M., Peng, L., Kroon, J., Bourgeois, D. & Goeldner, M. (2001) *Chem. Biochem.* **2**, 845–848.
Stoddard, B. L. (2001). *Methods*, **24**, 125–138.
Stoddard, B. L., Cohen, B. E., Brubaker, M., Mesecar, A. D. & Koshland, D. E. Jr (1998). *Nature Struct. Biol.* **5**, 891–897.
Stoddard, B. L., Koenigs, P., Porter, N., Petratos, K., Petsko, G. A. & Ringe, D. (1991). *Proc. Natl Acad. Sci. USA*, **88**, 5503–5507.
Sussman, J. L., Harel, M., Frolow, F., Oefner, C., Goldman, A., Toker, L. & Silman, I. (1991). *Science*, **253**, 872–879.
Teng, T.-Y. & Moffat, K. (1998). *J. Appl. Cryst.* **31**, 252–257.
Teng, T.-Y., Šrajer, V. & Moffat, K. (1994). *Nature Struct. Biol.* **1**, 701–705.
Ursby, T. & Bourgeois, D. (1997). *Acta Cryst.* A**53**, 564–575.
Walker, L. J., Moreno, P. O. & Hope, H. (1998). *J. Appl. Cryst.* **31**, 954–956.
Weik, M., Kryger, G., Schreurs, A. M. M., Bouma, B., Silman, I., Sussman, J. L., Gros, P. & Kroon, J. (2001). *Acta Cryst.* D**57**, 566–573.
Weik, M., Ravelli, R. B. G., Kryger, G., McSweeney, S., Raves, M. L., Harel, M., Gros, P., Silman, I., Kroon, J. & Sussman, J. L. (2000). *Proc. Natl Acad. Sci. USA*, **97**, 623–628.